

SECOND GENERATION OF FREE-FLYING MAGNETOMETER: SYSTEM ON A CHIP IMPLEMENTATION*

Brent Blaes, Hamid Javadi, Linda M. Miller, Beverly Eyre, and Udo Lieneweg
Jet Propulsion Laboratory
California Institute of Technology
Pasadena, CA

ABSTRACT

A Free-Flying Magnetometer (FFM) is an autonomous spin-stabilized "sensorcraft" that measures vector magnetic field at dc and low frequencies by means of a 3-axis magnetometer. Multiple FFMs are deployed to provide synchronized multipoint magnetic field measurements. These kinds of measurements are enabling new science by determining the fine-scale structure of the currents in the ionosphere involved in the production of aurora (auroral current is caused by penetration of energetic electrons in the solar wind that are accelerated by the Earth's magnetic field and resulting in the outward escape of ions). The Jet Propulsion Laboratory (JPL) recently developed a "hockey puck" FFM using Commercial Off The Shelf (COTS) technology. This FFM design was successfully demonstrated as part of the Enstrophy sounding rocket mission. This paper discusses the first generation hockey-puck FFM and its planned future development. A second generation FFM design targeted at further miniaturization and enhancements in functionality are possible through the use of monolithic magnetometers, Systems On A Chip (SOAC) technology, and advanced packaging.

FIRST GENERATION FFM

Four "hockey puck" (80 mm diameter, 38 mm height, 250 gram mass) FFMs, Fig. 1, were successfully ejected from the payload of a sounding rocket launched from Poker Flats, Alaska on February 11, 1999¹. The FFMs measured the vector magnetic field at 4 points separate from the payload at relative distances up to 3 km, and communicated their data, in bursts, to the ground. The Enstrophy sounding-rocket mission was a collaborative project between the University of New Hampshire, Cornell University and JPL. The science goal of the mission was the study of

current filamentation phenomena in the Earth's northern auroral region through multipoint measurements of magnetic field. Any three direct, unambiguous measurements of the local magnetic field allow one to calculate the local current density, J , by computing the curl of the magnetic flux density ($J = \nabla \times B/\mu_0$). The technical objective of the mission was the proof of concept of the JPL FFM design and demonstration of the synchronized in-situ multipoint measurement technique employing multiple free-flying sensorcraft. A photograph of the "Hockey Puck" FFMs that were utilized on the Enstrophy mission is shown in Fig. 1. These FFMs are designed to be ejected from the rocket payload spinning on their axis at around 11 Hz. A 3-axis flux-gate magnetometer sits in the center of the hockey puck. Each axis has a measurement range of $\pm 60,000$ nT and a resolution of less than 2 nT. The x- and y-axis are in the spin plane while the z-axis is along the spin axis. The symmetrical, balanced hockey-puck form factor provides spin-stabilization and facilitates a simple sciencecraft spin removal procedure for obtaining vector magnetic field from 3-axis magnetometer data.

The hockey-puck FFM utilizes a synchronized four-channel delta-sigma ($\Delta\Sigma$) Analog-to-Digital Converter (ADC) configured to sample at a rate of 279 conversions/sec, which sets the cutoff frequency at 73 Hz and sets the useable dynamic range to 108 dB or slightly more than 17 bits (1.144 nT/bit) resolution. The fourth ADC channel is multiplexed for system health monitoring of four temperature sensors and two battery voltages. The FFM also contains two sun sensors, a laser diode which emits a fan-shaped beam, a miniature S-band transmitter for direct communication to the ground station antennas, an ultra-stable Temperature Compensated Crystal Oscillator (TCXO) clock, an integrated data subsystem² implemented with a Field-Programmable Gate Array (FPGA), a 4 Mbit

* Copyright © 1999 by the American Institute of Aeronautics and Astronautics, Inc. The U.S. Government has a royalty-free license to exercise all rights under the copyright claimed herein for governmental purposes. All other rights are reserved by the copyright owner.

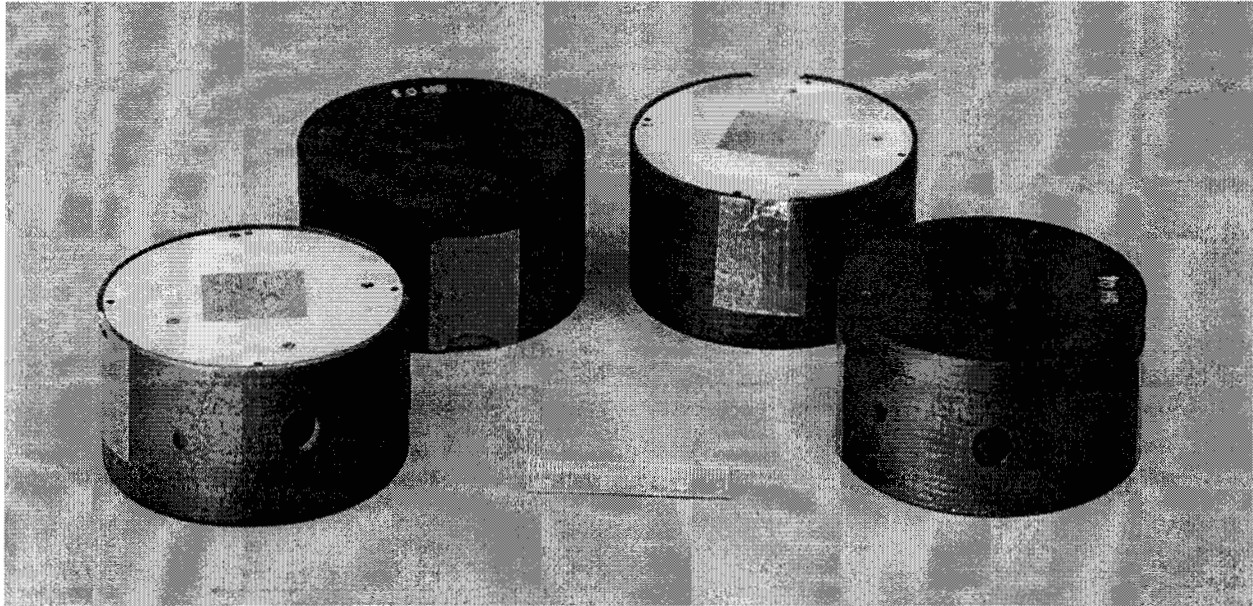


Fig. 1. "Hockey puck" FFMs that flew on Enstrophy sounding rocket mission. This photograph was taken after final vibration tests. The metal foil tape covering the sun sensors seen on FFMs 1, 2, and 3, counting from left to right, was removed before flight. Patch antennas are facing up on FFMs 1 and 3 while the tape-covered IR photodiode openings are facing up on FFMs 2 and 4. The large openings seen on the sides of FFMs 1 and 4 house a laser beacon, while the small openings are for out-gassing during launch.

Static Random Access Memory (SRAM) for data storage and high-capacity Lithium Thionyl Chloride (Li/SOCl₂) batteries for power. Communicating commands to the FFM prior to deployment is achieved with an infrared (IR) link. The FFM IR receiver responds to 9-bit pulse coded signals that are generated by an IR Light Emitting Diode (LED) in the payload for turning FFM power on or off and placing the FFM in a test mode or flight mode. The IR links are also used to synchronize (zero) the clocks onboard all the FFMs through a reset pulse originating from the payload GPS receiver that is issued when the FFMs are in flight mode. The FPGA-based data subsystem manages continuous data collection from the four ADC channels and sun sensors, formatting and storing the data to SRAM, and controlling downlink transmission. The transmitter is powered only after a 2547 frame SRAM buffer has been filled (~ 5 minutes of data). The data is Viterbi encoded and sent to the S-band transmitter via a First-In-First-Out (FIFO) buffer whose output is clocked at 100K bits/second. After the 26-second total transmission time, the transmitter is turned off to reduce noise coupling to the sensitive magnetometer. The data subsystem control consists of a master state machine that performs data flow management and is interfaced through a prioritized interrupt scheme to state machines that service the ADC, sun sensors and transmitter FIFO. Continuous data collection prevents the loss of data

during transmission and provides implicit time tagging of the data acquired by the ADC because of synchronization with the TCXO clock.

The hockey-puck FFMs are housed in graphite composite shells with a patch antenna lid. The low electrical resistance of the graphite minimizes eddy currents and prevents electrostatic charging. The antennas are centered on the FFM spin axis and can be seen in Fig. 1 on FFMs 1 and 3, counting from left to right. An opening for an IR photodiode, used for an optical umbilical command link, is on the spin-axis at the center of the shell opposite the patch antenna. These are seen, covered with tape, in Fig. 1 on FFMs 2 and 4. The hockey-puck FFMs were designed for a short sub-orbital flight. The FFM flight experiment lasted for 15 minutes after ejection from the payload at an altitude of ~300 km. During the FFM flight, which reached an altitude of 1071 km, three 5 minute data segments were acquired and transmitted in 26 second bursts to the 11-meter dish at Poker Flat. These FFMs were built using off-the-shelf commercial, industrial, and military grade surface-mount electronic components. Radiation-hard electronics was not required for this short sub-orbital flight. One of the primary technical challenges faced in developing the electronics for this FFM was minimizing electric and magnetic noise and its coupling to the sensitive integrated fluxgate magnetometer.

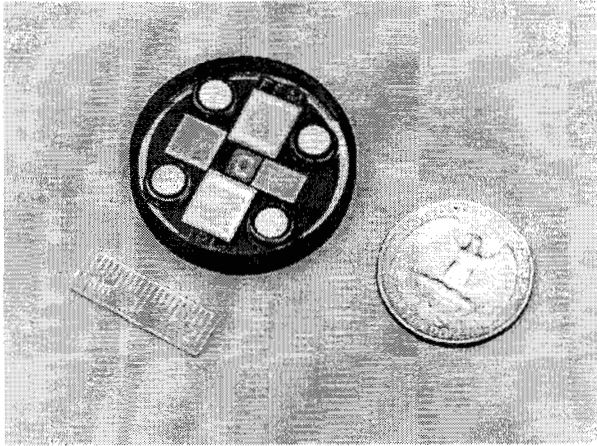


Fig. 2. Conceptual "Silver Dollar" FFM

Electronic components were screened for minimal magnetic signature. Coupling was minimized through shielding, demagnetizing magnetic materials in packages and lead frames, minimizing the areas of current loops, and compensating offsets with properly positioned dc current loops.

SECOND GENERATION FFM CONCEPT

The first-generation hockey-puck FFM was a proof-of-concept design developed to obtain magnetic measurements through the earth's magnetosphere and ionosphere in the northern Auroral zone. A reliable radiation-hard second generation FFM would be designed for long-term planetary missions to investigate magnetospheric field configurations in regions having small-scale structure and to separate spatial and temporal variations. A fleet of short-lived (expendable) FFMs would be deployed into a targeted region to gather multiprobe vector magnetic data. The FFMs would be ejected from the parent spacecraft at a speed of a few m/sec and would cover spatial volumes of order tens of kilometers for times of order one hour. The parent spacecraft would carry a sufficient number of FFMs for multiple deployments. The model shown in Fig. 2 is that of a conceptual second-generation FFM. This "silver dollar" FFM is implemented as a multi-chip module. As such, this is not a system on a "single" chip but would utilize proven system-on-chip technology. A future implementation (i.e. 3rd generation) may be fully contained on a single chip. The conceptual 2nd generation FFM shown in Fig. 2 contains an integrated 3-axis magnetometer consisting of three magnetic sensors functionally oriented in an orthogonal triad that sits at the center of the FFM surrounded by analog/mixed-signal, digital, memory,

and transmitter chips. Components are placed to distribute the mass and to assure dynamic balance along the spin axis. The more massive components (ie batteries) are placed along the outside rim to maximize the moment of inertia along the spin axis. Miniaturizing the FFM is not the only goal, but also to improve its reliability and radiation tolerance, and lower cost. The cost effective fabrication and integration levels achievable with semiconductor technology can enable the realization of these goals. As a side benefit, the monolithic integration of sensor and interface electronics can enable better performance like reduced drift, lower power consumption, and reduced parasitic effects. Fig. 3 is a graphical display of volume, mass, power, parts count, and recurring cost that contrast the hockey-puck FFM with goals set for the silver-dollar FFM.

FFM SYSTEM ARCHITECTURE

The essential components utilized in the first generation FFM are also required in the second generation design. They are: 1) a sensitive 3-axis magnetometer; 2) synchronized 3-channel Analog-To-Digital (ADC) converters having high linearity and resolution, low noise, and high channel-to-channel isolation; 3) an accurate clock having low drift and temperature dependence that is used to determine the attitude (position and orientation) of the FFM; 4) sun/star sensor used in conjunction with the clock for determining the spin orientation of the FFM; 5) Radio-Frequency (RF) transmitter to relay data to parent spacecraft or landing craft on the surface of a planet; 6) a wireless umbilical interface used to communicate with the FFM prior to deployment; 7) a data subsystem for acquiring, formatting, and storing data in memory

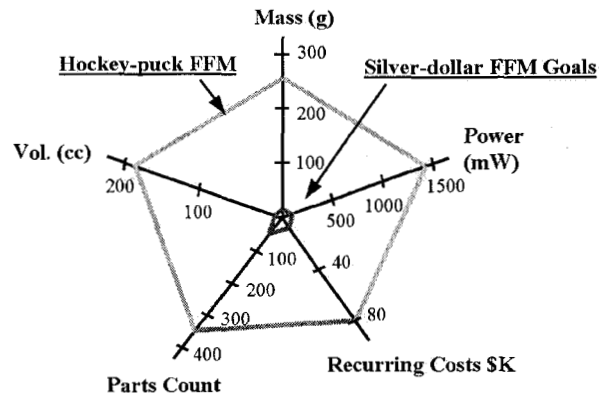


Fig. 3. Key metrics that contrast the hockey-puck FFM with goals set for the silver-dollar FFM

and controlling power and downlink transmission; and 8) power source with conditioning and management, electronics.

An FFM system block diagram, showing the interconnection of the eight components mentioned above, is illustrated in Fig. 4. The data subsystem manages continuous magnetometer data collection from three synchronized high-resolution ADCs, data from two sun sensors, and data from an ADC dedicated to system health monitoring. Data is communicated to the deploying parent spacecraft via a RF transmitter whose carrier frequency is programmable prior to deployment. The hockey-puck FFM communicates to the ground (Earth) using a lid-mounted patch antenna with a peaked radiation pattern normal to the FFM spin plane. An antenna with an omnidirectional radiation pattern is desired to enable robust angle-independent communication with the deploying spacecraft. Communicating to the FFM from the parent spacecraft prior to deployment is accomplished with an optical or capacitance coupled umbilical interface. The hockey-puck FFM contains a unidirectional optical interface utilizing an infrared photodiode in the FFM and light-emitting diode in the parent spacecraft. This interface is used to turn-on/off the FFM power, place the FFM in flight or test mode, and synchronize the FFM clock with the parent spacecraft clock. The 2nd generation umbilical interface will also support a calibration mode and the programming of parameters such as transmitter carrier frequency, FFM identification, and data downlink buffer size. Data and parameter read-back could be supported with a capacitance-coupled

bidirectional interface. An energy storage device such as a rechargeable battery or super capacitor that are able to withstand the extreme environments of space could supply FFM power. Super capacitors having capacitance densities exceeding 30 farads per gram of activated carbon and able to store energies in excess of 1.5 Joules per cubic centimeter are currently available³. The FFMs could be stowed in a non-powered state on the parent spacecraft until time of use (i.e. 10 years from Earth launch). This can prevent possible charge-related power-source leakage and degradation. This may not be a problem for some lithium based primary batteries that offer long storage time due to a passivation layer that is generated on Li electrodes. The FFM energy-storage device could be charged through a pair of recessed electrical connector pins or through the use of an inductive pickup coil in the FFM. The pickup coil would be open circuited after charging the energy-storage device to prevent fields generated by induced currents from effecting the fields being measured by the magnetometer sensors. Communication through the umbilical would commence after successfully charging the FFM. First, system and mission parameters would be uploaded. These would include transmitter carrier frequency, FFM identification, downlink buffer size, and magnetometer range and data rate. Next a test-sequence would be performed to verify RF transmitter operation, system voltages and temperatures. A magnetometer gain calibration would then be performed utilizing fields generated by coils on the parent spacecraft. This data would be compared against

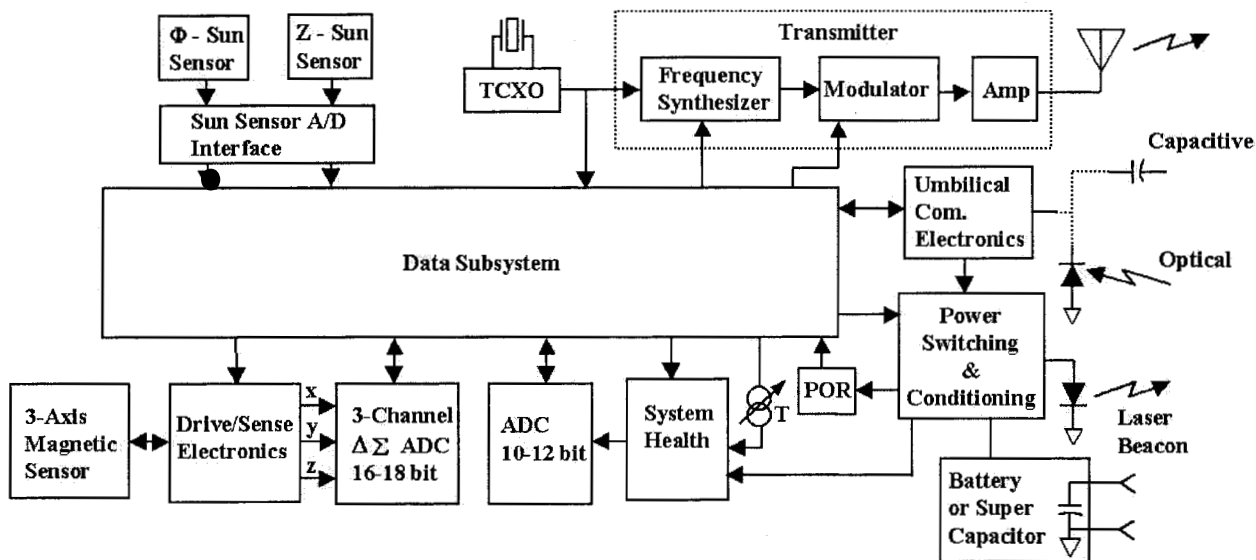


Fig. 4. Block diagram of FFM system

4

the pre-flight calibration data and used to baseline the FFM flight data. Finally, the FFM clock would be synchronized with the parent spacecraft clock and the FFM deployed. This procedure may be performed on a group of FFMs prior to clock synchronization and deployment.

FFM DATA SUBSYSTEM

The data subsystem in the hockey-puck FFM is implemented with hard-wired digital logic using a Field-Programmable Gate Array (FPGA). Sequence and control is accomplished with a master state machine that talks through prioritized handshake interfaces to other state machines that are in turn interfaced to system resources (ADC, transmitter, etc.). Therefore the functionality of the system cannot be changed.

Fig. 5 illustrates a second-generation FFM data subsystem that provides more flexibility through programmability. It would utilize a microcontroller core (i.e. 8051) and accommodate programmability by uplinking parameters and code through the umbilical

communication interface. The digital logic, comprising the data subsystem shown within the dashed box in Fig. 5, would be fabricated on one silicon chip. Circuitry contained in blocks outside the dash line in Fig. 3 consists of analog and mixed-signal electronics. For the silver-dollar FFM, this circuitry would be fabricated on a separate chip in order to utilize a low-noise mixed-signal fabrication process. Attempts would be made to integrate all electronics onto a single chip for future-generation FFM systems.

MAGNETIC FIELD SENSORS

The silver-dollar FFM is targeted to measure planetary magnetic field systems where a wide dynamic range ($> \pm 2000$ nT) and medium sensitivity (< 10 nT resolution) is required.⁴ Selecting the magnetometer sensor for this application is a primary issue driven by size, resolution, dynamic range, stability, power, reliability and compatibility with semiconductor processing. Interplanetary magnetic fields which vary over a narrower range of about 1 nT to 30 nT⁵ would require high resolution (< 100 pT) magnetometers (i.e.

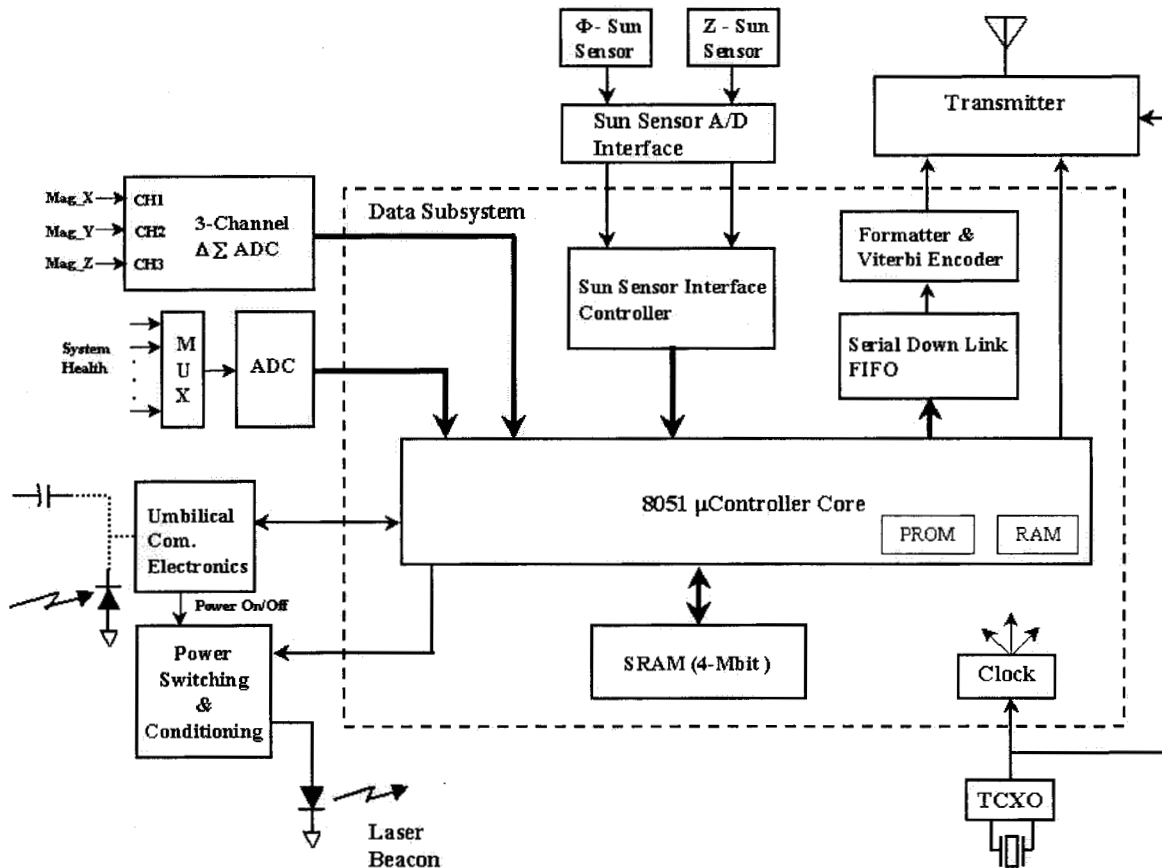


Fig. 5. Block diagram of microcontroller-based data subsystem.

5

vector helium magnetometer) for measurement. These magnetometers would be onboard the parent spacecraft and be utilized during the cruise phase to destination planets.

The fluxgate sensor is probably the most versatile vector magnetic field sensor^{6,7} because of its small size, low power requirements and reasonably good performance (sensitivity, dynamic range, and low noise). Fluxgate sensors can, however, have problems with high drift and temperature variations. The fluxgate sensor consists of a core composed of soft, high-permeability magnetic material that is periodically saturated by an excitation field which is in turn generated by a winding driven with an excitation current. The change in the core permeability modulates the flux in the core due to the external field being measured. A voltage proportional to the measured field intensity is induced in a sensing coil at the second (and higher) harmonic of the excitation frequency.⁸ The most common method for processing the sensor signal is to utilize a phase sensitive detector, usually preceded by a bandpass filter, to synchronously detect the second harmonic component of the sensor output voltage.

The hockey-puck FFM utilizes a miniature 3-axis fluxgate sensor consisting of one toroidal core, with orthogonal sense-coil windings for X and Y axis, and one race-track shaped core placed in the middle of the toroidal core with a single coil winding along the Z axis¹. The cores were made of a nickel-vanadium-iron alloy ($\text{Ni}_{83}\text{V}_6\text{Fe}_{11}$) with superior noise properties. This magnetometer has a sensitivity of 30,000 V/T, < 0.06 nT/ $\sqrt{\text{Hz}}$ noise, 100 Hz bandwidth, and 180 mW system power consumption. The overall dimensions of the sensor triad is 13 x 13 x 16 mm. This large "sugar cube" sized sensor will not fit into the silver-dollar FFM.

Fluxgates integrated on a CMOS chip with sensor supply, readout, and signal processing electronics have been demonstrated⁹ with 9200 V/T sensitivity, 30 nT/ $\sqrt{\text{Hz}}$ noise, 300 Hz bandwidth, and 160 mW system power consumption. A modified double metal CMOS process incorporating a 0.46 μm thick nickel-iron alloy ($\text{Ni}_{89}\text{Fe}_{19}$) was utilized. For this sensor to be a viable candidate for the silver-dollar FFM, the noise and power consumption must be reduced. This could be achieved by refining the process to accommodate a lower-noise magnetic material and tighter coupling of the coil windings to the sensor core.

Simple magnetoresistive sensors have achieved sensitivities on the order of 100 V/T at noise levels of 10 nT_{p-p}.¹⁰ Long-term temperature stability however is a problem with magnetoresistive sensors. Fluxgate-based magnetic field sensors, in comparison to magnetoresistance sensors, have the potential for lower

noise, and when operated with feedback for zero field operation, exhibit high linearity and high temperature stability.¹¹

Among magnetic-field sensing devices without magnetic material, Schottky magnetodiodes¹² have shown sensitivities of 30 V/T. These unique devices have been fabricated with a Silicon-On-Sapphire (SOS) process. The magnetodiode is simply a long p-i-n diode biased in the forward direction to achieve injection of holes and electrons from the p- and n-terminals into the intrinsic (-i-) region. A magnetic field applied in the plane of the SOS chip, perpendicular to the current, causes electrons and holes to experience a vertical deflection by the Lorentz force. When there is an asymmetry in the recombination rate between the top and bottom silicon film interfaces, the overall current in the device is affected accordingly. Further improvements in sensitivity and demonstration of low drift, low noise, and radiation immunity are required before this sensor can be utilized in the FFM application.

High sensitivity is also attributed to Micro-Electrical-Mechanical-System (MEMS) type devices. Two different MEMS magnetic sensors, both based on measuring the vibration amplitude of a mechanical Lorentz force oscillator, are being considered for the FFM application. One detects the vibration using an electron tunneling transducer¹³ and the other using a piezoresistor.^{14,15} Recently, a prototype electron-tunneling-based sensor has achieved a sensitivity of 3.15 V/T and noise of 6 $\mu\text{T}/\sqrt{\text{Hz}}$ when excited with a 10 mA 200 Hz current.¹³ This prototype sensor does not meet the requirements needed for the FFM but device performance models indicate that an optimized design is achievable for the FFM application. A cross-section of the MEMS-based magnetometer with tunneling transducer and interface electronics is shown schematically in Fig. 6. This device consists of a flexible, low-stress silicon nitride membrane (2.5 X 2.5 mm^2) and an opposing fixed, silicon, electron tunneling and electrostatic actuator. A voltage applied to the electrostatic actuator electrode pulls the flexible membrane to within ~ 10 Å of the tunneling tip enabling a nominal tunnel current of ~ 1 nA. Deflection of the membrane from the Lorentz force generated on the current-carrying coil generates a change in the tunnel current. This change is converted to a voltage that is summed to the deflection electrode voltage to counterbalance the Lorentz force and maintain the nominal tunneling current. A Wide dynamic range (>100 dB) is typical with this force-rebalance feedback configuration. The noise of this magnetometer is the excitation-frequency-sampled noise of the tunneling transducer's 1/f noise spectrum.

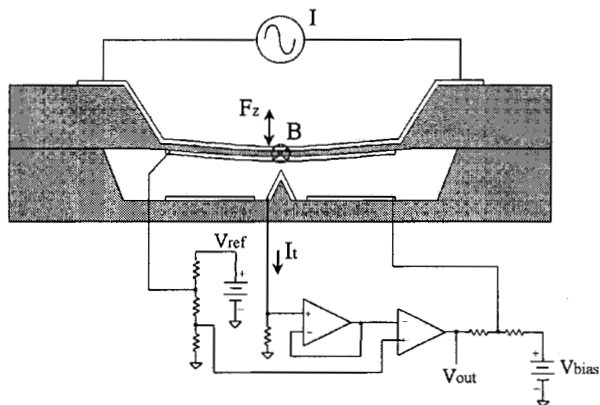


Fig. 6. Schematic diagram of electron tunneling magnetometer. Perpendicular component of magnetic field, B , to membrane current, I , produces a Lorentz force F_z on membrane. The membrane deflection changes the tunneling current, I_t . A control voltage is generated from this current that electrostatically deflects the membrane in the opposite direction, thus reducing the current change to nearly zero.

By increasing the current excitation frequency from 200 to 1000 Hz, a 3.3 X improvement in noise is produced. Further, by increasing the number of loops of wire on the membrane from 1 to 30, increasing the dimensions of the membrane to $5 \times 5 \text{ mm}^2$, and increasing the excitation current to 33 mA, a 700X cumulative improvement in the noise is predicted ($4 \text{ nT}/\sqrt{\text{Hz}}$), enabling this sensor for the FFM application.

A MEMS-based resonant magnetic sensor utilizing piezoresistors is also under consideration for the second generation FFM as a novel device implemented in a standard CMOS process with a single post-fabrication etching step.^{14,15} This sensor exhibits small size ($< 1 \text{ mm}^2$), thermal insensitivity, low power ($< 1 \text{ mW}$), and programmable dynamic range. The sensor consists of an oxide plate suspended by two sets of L-shaped support beams over an etched cavity as shown in Fig. 7. One of the beams contains two polysilicon piezoresistors for sensing minute rotational deflections (rocking) of the plate while the other provides access for bringing a metal loop onto and off from the plate. The loop encircles the plate around its perimeter and is excited with a sinusoidal current which interacts with the magnetic field producing a force which acts on the plate. A schematic of the plate-beam system is illustrated in Fig. 8. A pair of unstrained polysilicon resistors in thermal equilibrium with an active pair form a Wheatstone bridge. The bridge transduces the strain-induced change in resistance into a change in voltage. The unamplified sensitivity of this sensor depends on the magnitude of the sinusoidal excitation current and on the voltage or current that

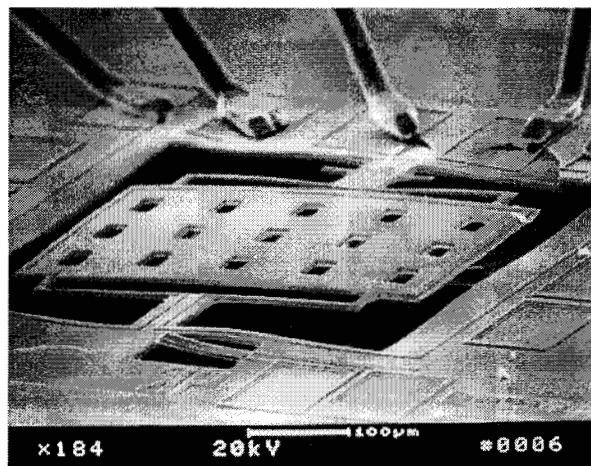


Fig. 7. Scanning electron micrograph of piezoresistor based resonant magnetic sensor.

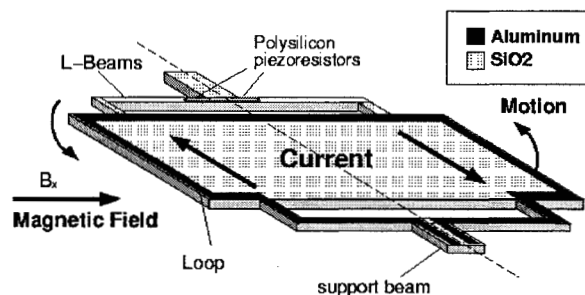


Fig. 8. Schematic of plate-beam system of piezoresistor-based resonant magnetic sensor.

powers the Wheatstone bridge circuit. As with the electron tunneling magnetometer, force-rebalance feedback can be utilized to enhance linearity and dynamic range.

Tests performed on the submillimeter-sized sensor (Fig. 7) over a range of 0 – 35 mT have successfully been used to validate an electromechanical sensor model. The model can be used in the design of an optimized application-specific (i.e for FFM) magnetic sensor. Modeling and tests have confirmed that, when running the sensor at the resonant frequency of the mechanical system, the sensitivity is multiplied by the quality factor Q and that sensitivity can be enhanced without giving up resolution. Assuming thermal noise in the piezoresistors as the ultimate limitation of resolution for this sensor, future design improvements are predicted to yield $1 - 10 \text{ nT}/\sqrt{\text{Hz}}$ performance.¹⁵ A fully integrated 3-axis sensor is currently under development, which if optimized to

meet predicted performance goals would satisfy the FFM application requirements.

FFM IMPLEMENTATION ISSUES

Minimizing the effects of live circuitry in close proximity to the magnetic field sensors is a major challenge. The fields generated by currents flowing in the FFM circuitry can introduce offsets and considerable noise. The approach utilized in the hockey-puck FFM to minimize this effect at the circuit-board level (minimizing the areas of current loops by utilizing two overlapping circuit-board layers) need to be applied at the chip level. For integrated devices advance simulation of stray fields becomes even more important. The concept of calculating fields from conductors using Biot-Savart's law was demonstrated in the design of PCBs for the first FFM. In addition, noise coupling caused by the coexistence of weak analog and strong digital signals in close proximity can become the limiting factor to overall measurement resolution. The sensors, their analog detection and conditioning circuitry and the ADCs are most vulnerable to digital switching noise, resistively coupled substrate noise, and capacitive coupling between interconnects. The performance of a mixed-signal chip will depend, to a large extent, on the design methodology capable of decoupling digital and analog parts. Noise coupling may be minimized by employing low-noise-emitting digital circuit techniques, isolating grounds and decoupling power, by layout-based isolation (keeping high-level signals away from high-gain inputs through separation and shielding), and utilizing noise-insensitive analog processing (i.e. differential-mode, carrier-based signaling with noise-rejecting carrier locked phase-sensitive detection, etc.).

CONCLUSIONS

The successful implementation and flight of the hockey-puck FFMs offers a solid base from which the 2nd generation silver-dollar FFM can be developed. Miniaturization of the FFM electronics through high levels of integration on a few silicon chips is presently realizable. The development of a 3-axis magnetic field sensor meeting the FFM application requirements is the greatest challenge. Several prospective sensor technologies were presented in this paper.

Future FFM designs (i.e. the size of a quarter) would rely on much higher levels of integration. Here the bulk of the system would be fabricated on a single chip using a standard commercial semiconductor process. Post processing would be utilized to form devices (i.e.

sensors, on-chip power, embedded passives, etc) that are not compatible with the standard process. Other nonsilicon parts (i.e. laser, GaAs transceiver, etc.) would be physically and electrically attached to the silicon chip forming a single monolithic system.

ACKNOWLEDGEMENT

The work described in this paper was carried out at the Jet Propulsion Laboratory, California Institute of Technology, under a contract with the National Aeronautics and Space Administration."

REFERENCES

- 1 H. Javadi, B. Blaes, M. Boehm, K. Boykins, J. Gibbs, W. Goodman, U. Lieneweg, J. Lux, K. Lynch, P. Narvaez, M. Quadrelli, D. Perrone, B. Snare, H. Spencer, M. Sue, B. Thoma, J. Willis, J. Weese, K. Leschly, and R. Goldstein, First-Generation Jet Propulsion Laboratory Hockey-Puck Free-Flying Magnetometers for Distributed In-Situ Multiprobe Measurements of Current Density Filamentation in the Northern Auroral Zone: Enstrophy Mission, *2nd International Conference on Integrated Micro/Nanotechnology for Space Applications*, April 11-15, 1999.
- 2 B. Blaes, Hamid Javadi, H. Spencer, Free-Flying Magnetometer Data System Architecture and Hardware Realization Using Commercial Off the Shelf (COTS) Technology, *To be presented at the 18th Digital Avionics Systems Conference*, October 23-29, 1999
- 3 Evans Capacitor Company:
<http://www.evanscap.com>
- 4 M. Kivelson, K. Khurana, J. Means, C. Russell, and R. Snare, The Galileo Magnetic Field Investigation, *Space Science Reviews* 60: (Kluwer 1992) 357-383.
- 5 A. Balogh, The Ulysses Magnetometer, *IEE Colloquium on Satellite Instrumentation*, (1988) 211-213.
- 6 G. Bartington, IEE Colloquium on Sensors for Low Level, Low Frequency Magnetic Fields (1994/096) 2/1 - 2/9.
- 7 J. Lenz, A Review of Magnetic Sensors, Proc. IEEE, (June 1990) 973 - 989
- 8 P. Ripka, Review of fluxgate sensors, *Sensors and Actuators A*, 33 (1992) 129-141

- 9 R. Gottfried-Gottfried, W. Budde, R. Jähne, H. Kück, B. Sauer, S. Ulbricht, U. Wende, A Miniaturized Magnetic Field Sensor System Consisting Of A Planar Fluxgate Sensor And A CMOS Readout Circuitry, *8th Int. Conf. on Solid-State Sensors and Actuators and Transducers '95 Eurosensors IX*. Vol. 2 , (1995) 229 - 232.
- 10 P. Ripka , Alternating current-excited magnetoresistive sensor, *Journal of Applied Physics* 79: (8) (Apr 15, 1996) 5211- 5213
- 11 O. Dezuari, E. Belloy, S. Gilbert, and M. A. M. Gijs, New Hybrid Technology for Planar Fluxgate Sensor Fabrication, *IEEE Trans. on Magnetism*, Vol. 35, No. 4, (1999) 2111 – 2117.
- 12 S. Cristoloveanu and S.S. Li, *Electrical Characterization of SOI Materials and Devices*, (Kluwer 1995) 68-70.
- 13 L. M. Miller, J. A. Podosek, E. Kruglick, T. W. Kenny, J. A. Kovacich, W. J. Kaiser, A μ -Magnetometer Based on Electron Tunneling, *IEEE Proc. , 9th Annual International Workshop on Micro Electro Mechanical Systems, (1996) 467 – 472.*
- 14 B. Eyre, K. S. J. Pister, and W. Kaiser, Resonant Mechanical Magnetic Sensor in Standard CMOS, *IEEE Elec. Dev. Letters*, Vol. 18, No. 12 (Dec. 1998) 496 – 498
- 15 B. Eyre, K. S. J. Pister, Micromechanical Resonant Magnetic Sensor in Standard CMOS, *Transducers 97, 1997 Int. Conf. On Solid-State Sensors and Actuators, June 16-19, 1997. Vol 1, # 2B1.08P.*